UNIVERSITY OF CALIFORNIA SAN DIEGO

A Wireless, Reconfigurable, Multichannel Potentiostat for Wearable Electrochemical Biosensing Applications

A thesis submitted in partial fulfillment of the requirements for the degree

Master of Science

in

Electrical Engineering (Electronic Circuits and Systems)

by

Brian Lazaro Wuerstle

Committee in charge:

Professor Patrick Mercier, Chair
Professor Joseph Wang, Co-Chair
Professor Truong Nguyen

2021

The Thesis of Brian Lazaro Wuerstle is approved, and is acceptable in quality and form for publication on microfilm and electronically.

University of California San Diego

2021

TABLE OF CONTENTS

Thesis Approval Page iii
Table of Contents iv
List of Figures and Tables v
Abstract of the Thesis vi
Chapter 1 Introduction 1
Chapter 2 Electronics for Electrochemical Biosensing 3
Chapter 3 Design of a Reconfigurable Potentiostat 13
Chapter 4 Conclusion 38
References 39

LIST OF FIGURES AND TABLES

Figure 2.1. Functional block diagram of an electrochemical biosensing system 3
Figure 2.2. Example instrumentation circuits for electrochemical analysis. 4

Figure 3.1. CWS-Stat design overview. 15
Figure 3.2. Battery and charging coil integration with the CWS-Stat for wireless charging capability. 17
Figure 3.3. Electrochemical AFE configuration 18
Figure 3.4. BLE operation for the CWS-Stat. 21
Figure 3.5. Electrochemical method comparison between the CWS-Stat and commercial potentiostat 23
Figure 3.6. Input-referred referred noise for amperometry. 24
Figure 3.7. Current consumption of the CWS-Stat in amperometry mode 25
Figure 3.8. Integration of the CWS-Stat into wearable microneedle-based biosensing system. 28
Figure 3.9. On-body results of the microneedle-based electrochemical biosensing system. 29

Figure S3.1. Programming and reprogramming steps of the CWS-Stat 31
Figure S3.2. Autoranging system for amperometric measurements. 32

Table 2.1. Examples of ICs for Electrochemical Sensing 6
Table 2.2. Examples of BLE System-on-Chip and System-in-Package ICs 7

Table 3.1. Integration Time Thresholds for Square Wave Voltammetry 20
Table 3.2. Comparison of State-of-the-Art Potentiostats 27

Table S3.1. Gain Table 36
Table S3.2. LED Status Indicator Key 37

ABSTRACT OF THE THESIS

A Wireless, Reconfigurable, Multichannel Potentiostat for Wearable Electrochemical Biosensing Applications

by

Brian Lazaro Wuerstle

Master of Science in Electrical Engineering

University of California, San Diego, 2021

Professor Patrick Mercier, Chair

Professor Joseph Wang, Co-Chair

Wearable chemical sensing technology shows promise as a convenient method for continuously and non-invasively monitoring physiological parameters via biochemical markers such as glucose, lactate, and alcohol. Measuring these biomarkers from easily accessible biological fluids (e.g. sweat, saliva, and interstitial fluid) can provide a more comprehensive view of one's health and fitness compared to other biosensing techniques, such as motion sensing and electrophysiological signal recording. Extracting this physiochemical data in real-time is possible through wearable devices formed by integrating electrochemical biosensors with low power electronics. This thesis provides an overview of how these electronics are developed, presents a realized design, and demonstrates the design's successful integration with a wearable sensor to create an electrochemical biosensing system.

Chapter 1 Introduction

Wearable technology has recently emerged as a method for individuals to conveniently monitor their health and fitness [1], [2], typically by measuring physical data (e.g. motion) or electrical data (e.g. ECG waveforms) to do so. For example, a device may track the number of steps the user has taken or the number of calories the user has burned as metrics to measure fitness progression. Another is recording a user's electrocardiogram (ECG) in real-time to monitor for heart arrhythmias [3]. Though physical and electrical-based biosensing techniques have already seen adoption into commercial wearable devices, another category of sensing, chemical-based biosensing, has not yet seen such adoption. Monitoring chemicals such as glucose [4], sodium [5], lactate [6], alcohol [7], and levodopa [8] from easily accessible biological fluids (e.g. sweat, saliva, and interstitial fluid) can potentially provide individuals insight into their physiology from a perspective that is entirely different from what is allowed by motion sensing or electrophysiology alone, giving one a more comprehensive view of their health / fitness. For instance, real-time tracking of lactate in an athlete's sweat can be used to measure their physical exertion, and thereafter be used to procure an optimal training regimen [9]. Ultimately, there is an opportunity for chemical sensing via wearable devices to make a tremendous impact on health and fitness monitoring.

Given the utility in continuously tracking chemicals for health/fitness monitoring, on top of the recent emergence / consumer adoption of wearable devices, many advancements have been made towards developing wearable chemical sensors in recent years. One type of chemical sensors – *electro*chemical sensors – shows promise for wearable applications, particularly because they can be integrated into the electronic systems we commonly use today, namely smartphones wirelessly connected to wearables via Bluetooth. These sensors produce electrical signals proportional to chemical concentrations, which electronic instrumentation can measure, process, and subsequently transmit wirelessly to a smartphone for data capture and visualization. In addition to functionality (that is, the capability of measuring chemical concentrations), the electronics must also meet usability demands of wearable devices in terms of device

size and battery life. Thus, as wearable chemical sensor research continues to advance, so must the electronics which integrate with these sensors to ultimately create miniaturized, long-lasting devices.

The following chapters provide the reader an overview how the electronics for wearable electrochemical biosensing devices are developed. First, the design considerations for the electronics are described, followed by recent works in literature and research opportunities. Afterwards, a realized design is presented which aims to advance the current state-of-the-art research for chemical sensing electronics. Lastly, the design's integration with an electrochemical biosensor to create a wearable biosensing system is detailed, along with on-body test results to validate its operation.

Chapter 2 Electronics for Electrochemical Biosensing

2.1 System Overview

Wearable devices for fitness / health monitoring generally follow the same system architecture, consisting of: 1) a sensor or electrode(s) which interfaces with the body to sense physiological data (e.g. an accelerometer or gyroscope for transducing movement to electrical signals, or skin electrodes for capturing ECG signals), 2) electronics which can accurately and precisely measure the signals produced by the sensor / electrode, process those signals, and subsequently transmit measurement data, and 3) a mobile device to wirelessly receive the data. Figure 2.1 depicts this architecture adapted for electrochemical biosensors - sensors which transduce concentrations of a particular analyte / biomarker into an electrical signal. Signals are captured by a potentiostat circuit (an electronic instrument used to perform electrochemical analysis) then digitized via an analog to digital (A/D) converter. Data is then processed and finally transmitted to a mobile device (e.g. smartphone) for visualization. Additionally, each of these electronic blocks requires a power source to operate.

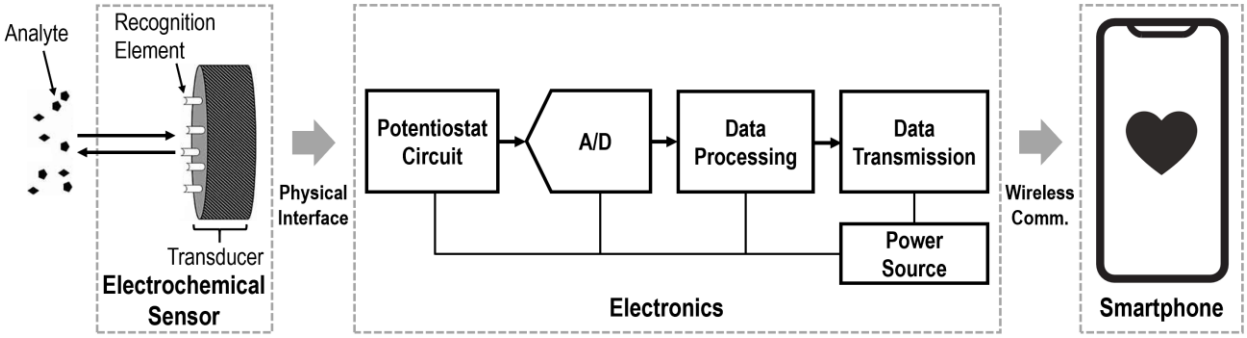

Figure 2.1. Functional block diagram of an electrochemical biosensing system, consisting of 1) an electrochemical sensor, 2) electronics for measurement data acquisition, processing, and transmission, and 3) a smartphone for data visualization.

The potentiostat circuit (Figure 2.2) used in the system will vary depending on the method of electrochemical analysis used with the sensor. Functionally, sensors operate as electrochemical cells which are composed of a working electrode (WE) and reference electrode (RE), as well as a counter electrode

(CE) for current-based electrochemical methods. Potential-based sensors (e.g. ion specific electrodes) produce potentials proportional to the natural log of chemical concentration (nernstian behavior) across the working and reference electrodes. To measure these potentials, the potentiostat circuit must present a high input impedance to the working electrode, which a simple voltage buffer can provide. Current-based sensors (e.g. enzymatic sensors), on the other hand, produce currents linearly porportional to chemical concentrations. This current is the cell's response to an applied potential (V_{REF} in Figure 2.2) across the working and reference electrodes. The counter electrode is utilized to maintain the potential of the reference electrode via electrical feedback. A low input impedance is presented to the working electrode to measure the currents, which a transimpedance amplifier provides.

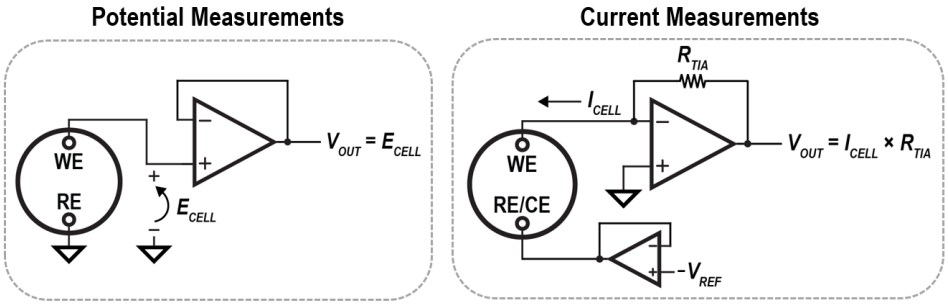

Figure 2.2. Example instrumentation circuits for electrochemical analysis.

2.2 Electronics Design Considerations

The design of the electronics for an electrochemical biosensing system can be split into a) component level design, which deals with the component selection for signal acquisition, processing, and transmission, as well as powering these components, and b) system level design, which deals with interfacing the electronics with other system elements, i.e. physically interfacing the electronics with an electrochemical sensor and wirelessly communicating with a mobile device.

2.2.1. Component Level Design

Each block of the electronics in Figure 2.1 must be implemented with a physical hardware component. Every component must not only perform its intended function, but must also facilitate device miniaturization and aid in low power operation. The conventional method for designing the electronics is to use the following components: a) integrated circuits for the potentiostat circuit, the analog to digital conversion, data processing, and for control of the data transmission; b) an antenna to support wireless operation; and c) a battery for powering these components. Additionally, all the components must be electrically interconnected, typically done on a rigid printed circuit board (PCB), though flexible substrates may be of use. The following sub-sections describe the considerations that must be taken for each of these components when designing an electrochemical biosensing device.

a. Integrated Circuits

Integrated circuit (IC) technology has enabled extreme miniaturization of electronic circuits, and a high level of integration of electronic systems, into packages measuring only a few square millimeters. Not only can each of the electronics blocks in Figure 2.1 be found within a commercially available IC (e.g. a microcontroller unit (MCU) for data processing or a BLE radio for data transmission), but multiple blocks can be found integrated under one package as a system-on-chip (SoC) (e.g. MCU *and* BLE radio together), affording even further miniaturization. Ideally, the components for the electronics would all be housed under a single IC package. No such IC, however, was commercially available at the time of

writing; yet, packages which contain the potentiostat circuit and ADC together, and ones which contain the MCU and BLE radio, can in fact be found commercially. It is therefore possible to implement the entire signal chain (from the potentiostat circuit to the data transmission block) using only two ICs. More information for each of these ICs are provided below. Note that in addition to miniaturization, latest IC technologies feature low power consumption owing to low quiescent current designs, reduced leakage, and the ability of the ICs to be placed into "sleep" modes in which circuits are effectively turned off via power gating / clock gating.

Potentiostat Circuit & ADC

Recent demand for ICs designed for electrochemical sensing has led to the integration of potentiostat circuit sub-components into one chip. A few of these ICs also integrate both the potentiostat circuit and ADC together, forming an electrochemical analog front end (AFE). Recent ICs may also feature multichannel inputs and signal conditioning circuits (i.e. analog/digital filters and amplification stages) which serve to improve the precision of measurements. Examples of these integrated circuits are provided in Table 2.1.

Table 2.1. Examples of ICs for Electrochemical Sensing

Components	Area [mm^2]	Year	Additional Features	Reference
Potentiostat Circuit	16.00	2011	-	[10]
Potentiostat Circuit & ADC	15.12	2019	Multichannel, Signal Conditioning	[11]
Potentiostat Circuit & ADC	8.63	2019	Multichannel	[12]

MCU & BLE Radio

The microcontroller unit (MCU) processes digital data from the ADC (e.g. converting ratiometric ADC readings to absolute electric potential readings) which is subsequently transmitted to a mobile device through a BLE radio. There are many commercially available ICs which integrate both the MCU and BLE Radio into a single package typically referred to as a "system-on-chip" (SoC). Integration of these components not only facilitates overall device miniaturization, but also facilitates low power

operation, as the inherent low communication latency between the integrated MCU and BLE radio can maximize time spent in sleep modes. Additionally, an antenna may be embedded into the package to form a system-in-package (SiP). Examples of commercially available BLE SoC and BLE SiP integrated circuits are provided in Table 2.2.

Table 2.2. Examples of BLE System-on-Chip and System-in-Package ICs

Components	Area [mm^2]	Year	Bluetooth Version	Reference	Comments
BLE SoC	25.00	2014	v4	[13]	-
BLE SoC	9.60	2017	v5	[14]	-
BLE SoC	5.50	2018	v5	[15]	-
BLE SiP	42.25	2014	v4	[16]	SiP version of [13]
BLE SiP	51.80	2017	v5	[17]	SiP version of [14]
BLE SiP	48.00	2018	v5	[18]	SiP version of [15]
BLE SiP	36.00	2020	v5	[19]	-

b. PCB Fabrication Technology & Materials

The components of the electronics must be soldered to a printed circuit board (PCB) to electrically interconnect them. Latest PCB fabrication technologies allow for compact designs in terms of area-density and height, with copper trace widths and copper spacing down to 3 mil (76.2 μm), board thicknesses down to 0.4mm, and up to 6 board layers for interconnections [20]–[22]. Though PCBs are typically made from rigid glass-epoxy based compounds, flexible polyimide-based (plastic) substrates are available as well [23], and can be utilized to flex /conform the electronics to the body in areas like the wrist, abdomen, and forehead.

c. Radio Antenna

Radio transmission of measurement data to a mobile device requires an antenna for operation. Antenna designs are chosen based on the application's size, range, and directivity requirements [24]. Printed antennas are particularly popular due to their low complexity and seamless integration with printed circuit board designs [25]. They can take many forms, such as microstrips, slot lines, and coplanar antennas [26], though the inverted-F antenna (IFA) is especially common for mobile device applications

for its low profile and an omnidirectional radiation pattern [27]. Printed antennas can also be placed onto flexible substrates [28], making them compatible with conformal electronics designs. Another widely used and compact antenna type is the ceramic chip antenna, which is generally smaller than most printed antennas at the cost of range and directivity. These chip antennas are typically assembled (soldered) to PCBs, though they can also be found embedded into SiP BLE modules.

d. Battery Technology

Battery technologies are typically characterized by their form factor, capability to be recharged, cell voltage, energy density, and shelf life, all of which are determined by the battery's material composition. Common materials are alkaline, nickel-metal hydride (NiMH), and lithium-ion. Form factor geometries include cylindrical, rectangular, coin shaped, or flat and thin. Certain battery technologies are even flexible, such as thin film lithium-ion batteries. These form factors should be leveraged for wearable device designs to meet the application needs. For example, a patch-like device would benefit from coin-cell or thin-film batteries which can minimize the total height of the device. Also, energy capacity for a given material generally increases with the physical size of the battery, so designs must be wary of trading off battery life for overall device size when selecting a battery.

2.2.2 System Level Integration

Integrating the electronics into a complete electrochemical biosensing system requires physically interfacing the electronics with an electrochemical sensor as well as a method of wirelessly transmitting data to a mobile device. Design considerations for both of these is discussed in the following subsections.

a. Physical Interface to Biochemical Sensor

The physical interface between the electronics and the electrochemical sensor should be chosen based on the mechanical properties of the chemical sensor. Recently, chemical sensors (namely sweat-based sensors) have been developed to conform to the body. These sensors typically utilize electrodes fabricated on flexible plastic substrates or temporary-transfer tattoos [29]. In these cases, electrodes can interface with the electronics via a zero insertion force (ZIF) or low insertion force (LIF) connector, maintaining electrical contact through printed / etched conductive traces on the substrate [30]–[32]. For a more permanent solution, the electronic components can be assembled directly onto the substrate rather than using a dedicated connector [33], at the expense of needing to dispose the electronics whenever the sensor ultimately degrades. Temporary-transfer tattoo sensors can be interfaced by pressing spring-based contacts, located on the electronics, onto conductive ink found on the sensor [34].

b. Wireless Communication Technologies

Wirelessly interacting with the electronics can be done through either radio communication technologies (long distance) such as Bluetooth or Wi-Fi, or near-field communication technologies (short distance) such as NFC or RFID. Radio communication has the advantage of allowing continuous, uninterrupted transmission of measurement data to a mobile device. However, radios consume a significant amount of peak power to sustain wireless links, and therefore require a battery for operation. Near field communication, on the other hand, allow power to be transferred wirelessly during interrogation, obviating the need for a battery. Unfortunately, the interrogation device (i.e. the user's smartphone) must hover directly over the wearable device every time measurement data needs to be acquired. The inconvenience of regularly performing this movement makes near field communication

impractical for continuously measuring data, thus making radio technologies preferred for these applications.

2.3 Recent Works & Opportunities

Novel electrochemical biosensor development hinges on precise and accurate electronics for capturing measurement data. Commercial, benchtop potentiostats – electronic instruments used for electrochemical analysis [35] – are typically utilized, as they are capable of high resolution and low noise measurements and offer a wide gamut of electroanalytical techniques (e.g. potentiometry, amperometry, square wave voltammetry). However, these commercial potentiostats do not meet the miniaturization demands necessary to be integrated with electrochemical biosensors to form wearable devices. Accordingly, there have been several lab-built, miniaturized potentiostats developed specifically to integrate with electrochemical biosensors to create wearable biosensing systems [30]–[33].

Most biosensing systems have utilized a single working electrode in order to detect a single analyte. Though these developments have significantly advanced the state of wearable chemical sensor research, measuring only a single analyte may not provide much information about one's fitness / health. To improve on these single analyte systems, devices which employ an electrode array for multi-analyte detection have been developed [31], [36]. Sensing from multiple working electrodes requires the electronics to be designed with components for both acquiring signals from the sensor (instrumentation and signal conditioning circuitry) and for multiplexing between the sensor's electrodes. Typically, this has been implemented either by having an independent potentiostat circuit (e.g. a transimpedance amplifier or voltage buffer) dedicated to each working electrode [37], or by multiplexing at the input of a single potentiostat circuit [38].

Up to now, developing the electronics for multi analyte detection with commercially available parts has required a number of discrete components (e.g. amplifiers for the potentiostat circuit, passives for signal conditioning circuits, and switches for multiplexing), resulting in large area designs which are not ideal for space constrained wearable devices. Recently, however, commercially available integrated circuits for electrochemical sensing have advanced to now include all of the circuits needed for multiplexed sensing operation, fitting them within a single package measuring only a few square

millimeters [11], [12]. Utilizing these ICs could drastically reduce the size of lab-built potentiostats relative to those designed with discrete components. Additionally, these ICs feature the circuitry for both potential-based and current-based electrochemical techniques, allowing them to be used with a wide gamut of sensor types (e.g. enzymatic sensors and potentiometry and ion specific electrodes). Therefore, the opportunity exists for one to leverage these recent advancements and develop a versatile, miniaturized potentiostat.

Given the growing number of wearable electrochemical biosensor technologies in literature, there would be great utility in a potentiostat which offers reconfigurability comparable to that of commercial potentiostats while still being small enough to be integrated with wearable electrochemical biosensors, in addition to advanced features such as multiplexed input selection and wireless operability. Such a device could enable rapid conversion of wearable electrochemical *biosensors*, which are typically bound to in-lab use only, into wearable, fully integrated electrochemical *biosensing systems*.

Chapter 3 Design of a Reconfigurable Potentiostat

3.1 Introduction

Current wearable electrochemical biosensors can detect biochemicals such as glucose, sodium, lactate, and alcohol. Acquiring measurement data from these sensors is performed through a potentiostat, the electronic instrument used for precise and accurate electrochemical analysis. Recently, miniaturized potentiostats have been developed to integrate with these sensors to create wearable devices used for measuring biochemical markers from tears, sweat, and saliva. Most of these potentiostats have been designed to sense only a single analyte from these biological fluids using a particular electrochemical technique (e.g. amperometry or potentiometry). However, these fluids typically contain multiple biomarkers, so it would be beneficial for a potentiostat to be able to sense multiple analytes. Given the growing number wearable electrochemical biosensors in literature, there would be much utility in a multichannel, multi-technique potentiostat which serves as a platform to perform multi-analyte detection with a variety of electrochemical biosensors.

Recent interest in chemical sensing technology has led to the advancement of commercially available integrated circuit (IC) technology used for electrochemical analysis. These ICs can perform both potentiometry and amperometry (and other controlled potential techniques), are capable of multichannel input switching, and are compact (measuring only a few square millimeters). Additionally, they consume µA levels of current, enabling long battery life operation. Altogether, the capabilities and size of these ICs make them perfectly suitable for wearable electrochemical biosensing systems.

This work leverages these recent advancements in integrated circuit technology to realize a wireless, battery-powered potentiostat, which features multiplexed inputs. It is capable of performing amperometry, potentiometry, and square wave voltammetry (on any input channel) to sense from a variety of electrochemical biosensors. Only a single IC is employed for multiplexed electrochemical sensing, thus improving upon previous works, which typically use multiple discrete components, in terms of area efficiency. The presented device is controlled via Bluetooth Low Energy (BLE) and features

wireless battery charging capability. This work is done towards advancing the state of wearable biosensing technologies by demonstrating a platform capable of being adapted to variety of electrochemical sensors to enable rapid development of wearable, fully integrated electrochemical biosensing systems.

3.2 Materials & Methods

3.2.1 Reagents and Chemicals

Phosphate buffered saline (PBS) hydrogen peroxide (H_2O_2), 3,4-dihydroxy-L-phenylalanine (L-Dopa), and sodium chloride (NaCl) were obtained from Sigma-Aldrich. All reagents and solvents were used without further modification and purification.

3.2.2 CWS-Stat Design

Component Overview

The CWS-Stat (Figure 3.1) features the AD5940 (AD5940BCBZ-RL, Analog Devices, Inc., Wilmington, MA, USA) electrochemical analog front end, the CYW20736S (CYW20736S, Cypress Semiconductor Corporation, San Jose, CA, USA) Bluetooth Low Energy (BLE) system-in-package (SiP) module, a 2.8V low-noise, low quiescent current low-dropout (LDO) regulator (LP5907UVX-2.8/NOPB, Texas Instruments, Dallas, TX, USA), a wireless Li-ion battery charger (LTC4124EV#TRMPBF, Analog Devices, Inc., Wilmington, MA, USA), a wireless charging coil (WR202020-18M8-G, TDK, Chuo City, Tokyo, Japan), and a 110mAh Li-ion coin cell battery (RJD2430C1ST1, Illinois Capacitor, Des Plaines, IL, USA). The electrode connection consists of 5 gold plated nickel, 0.508mm diameter pins (0508-0-00-15-00-00-03-0, Mill-Max Manufacturing Corporation, Oyster Bay, NY, USA).

All of the electronic components of the CWS-Stat are assembled onto a 4-layer FR4 printed circuit board (PCB) which measures 0.5mm in height and 5.3 cm^2 in area (r = 13mm). Fabrication and assembly were performed by PCBminions (Princeton, NJ, USA & Shenzhen, China). Components were purchased from Digi-Key Electronics (Thief River Falls, MN, USA).

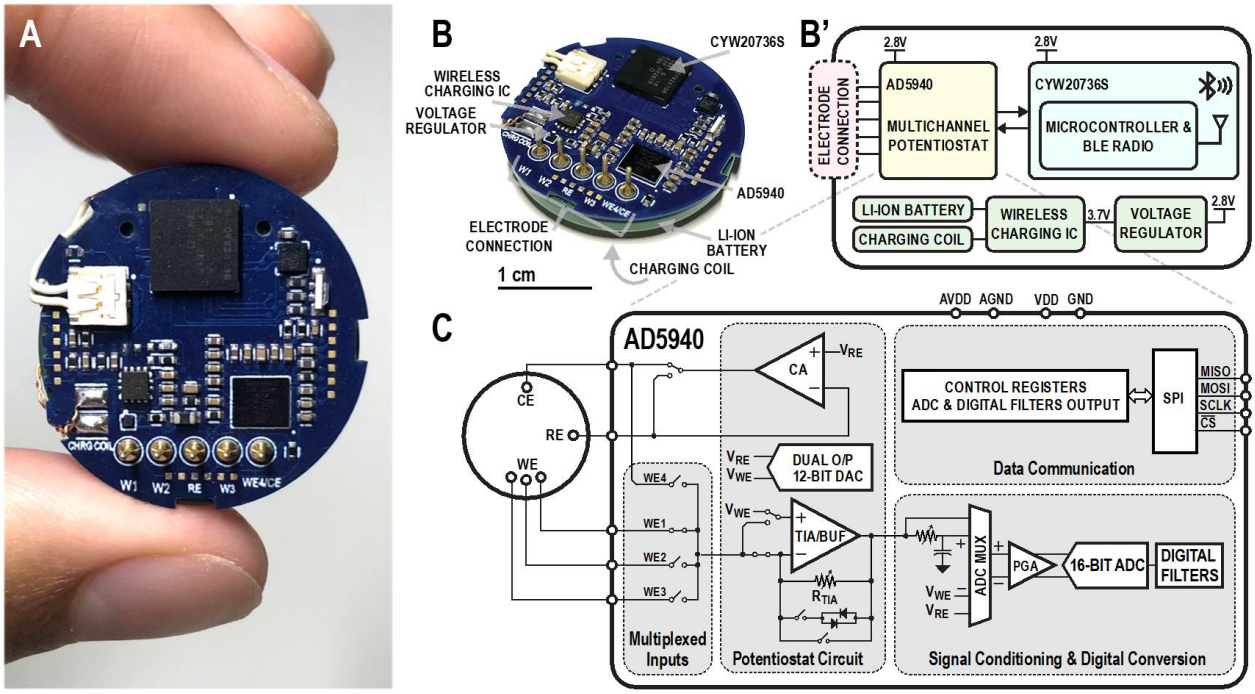

Figure 3.1. CWS-Stat design overview. (**A**) Photograph of the CWS-Stat. (**B**) Major components labeled on the CWS-Stat. (**B'**) Functional block diagram of the CWS-Stat's major components. (**C**) Abridged functional block diagram of the AD5940 AFE (recreated from the component's datasheet).

AD5940 - Electrochemical Analog Front End

The AD5940 is an electrochemical analog front end (AFE) which integrates multiple circuits for performing electrochemical analysis, all in one 3.6 x 4.2mm integrated circuit package. Figure 3.1C depicts the primary circuits found on the AFE used for electrochemical sensing, which can be functionally grouped into circuitry for multiplexed input selection, potentiostat operation, signal conditioning and digital conversion, and data communication.

There are 5 input/output pins used for electrochemical sensing on the AFE, four of which can be used as input channels in a 2-electrode configuration (labeled WE1, WE2, WE3, WE4), or three when used in a 3-electrode configuration (WE1, WE2, WE3). Each input can be digitally selected to connect to the potentiostat circuit for electrochemical analysis. Each of the 5 input/output pins is electrically connected to a single gold-plated electrode connector.

The potentiostat circuit consists of a control amplifier (CA), a TIA/BUF input amplifier which is configured to be either a transimpedance amplifier (TIA) for electric current measurements or a voltage buffer (BUF) for potential measurements, and a 12-bit digital-to-analog converter (DAC) to set the common mode reference electrode potential (V_{RE}) as well as the working electrode potential (V_{WE}) for controlled potential techniques. Signals from the TIA/BUF amplifier feed into the signal conditioning and digital conversion circuitry, which includes a programmable analog RC filter, a differential multiplexer (labeled ADC MUX), a programmable gain amplifier (PGA), a 16-bit, 800 kSPS analog-to-digital converter (ADC) for digitizing signals into measurement data, and a digital $sinc^3$ filter cascaded by a $sinc^2$ filter. Both the TIA and PGA feature programmable gain values.

The AFE also contains data registers to store configuration information and for storing measurement data from the ADC or digital filters. All data communication with these data registers occurs through the AFE's SPI interface.

CYW20736S – BLE SoC & Embedded Antenna

The CYW20736S features an ARM Cortex-M3 microcontroller (MCU), BLE radio, and an embedded planar inverted-F antenna, all within a 6.5 x 6.5mm package. The module is programmed to control all electronic system functionality of the CWS-Stat, namely configuration of the AFE through its SPI bus (e.g. multiplexed input selection, amplification / filter settings, control of the DAC), electrochemical measurement data acquisition, and wireless communication with a mobile device over BLE.

Programming the CWS-Stat is initially performed through a physical UART connection to a personal computer. Afterward, programming is done wirelessly via BLE through Over-the-Air (OTA) updates. This enables rapid deployment of firmware updates in line with today's agile software development environments. More information on the procedures for initial programming and reprogramming is provided in Supplementary Material 3.6.1.

Power Management and Wireless Recharging

The power management and wireless recharging circuitry on the CWS-Stat consist of a wireless recharger IC, a 2.8V LDO, and a wireless charging receive coil. Power for the electronics is sourced from the rechargeable Li-ion battery – a 2430 type (24mm in diameter, 3.0mm in height) coin cell. The electrical connectors for the charging coil and battery are shown in Figure 3.2A. The battery, receive coil, and PCB are adhered to each other with double-sided tape, resulting in a total device height (from the top of the battery connector to the bottom of charging coil) of 6mm and a diameter of 26mm (Figure 3.2B).

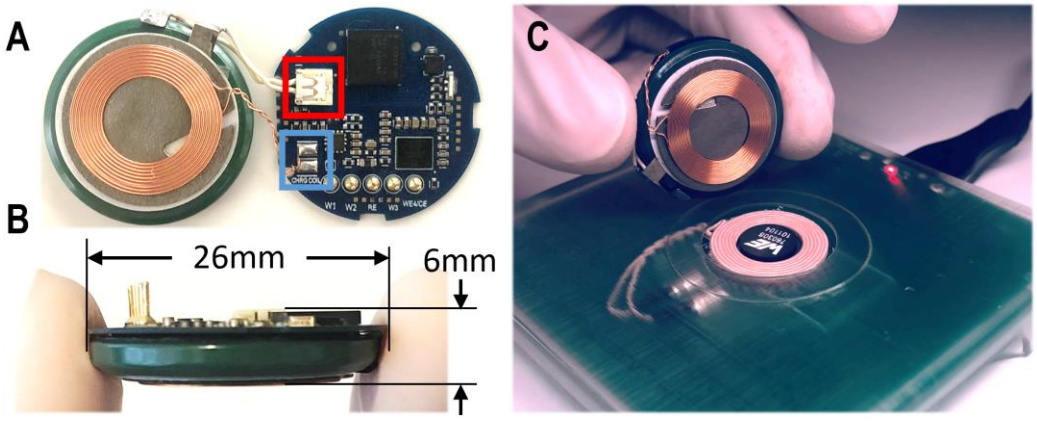

Figure 3.2. Battery and charging coil integration with the CWS-Stat for wireless charging capability. (**A**) CWS-Stat connection to the battery (red) through a low-profile connector (ACHR-02V-S and BM02B-ACHSS-GAN-TF(LF)(SN), J.S.T. Mfg. Co., Osaka, Japan) and charging coil (blue) through large solder pads. (**B)** Dimensions of the CWS-Stat with the battery and charging coil connected (not including the sensor connection). (**C)** CWS-Stat and transmitter pad (DC2771A-B WPT, Analog Devices, Inc., Wilmington, MA, USA) with coils to support wireless inductive power transfer.

Under normal operation, power is sourced from battery, through the wireless recharger IC, and into the LDO. The LDO then regulates the battery voltage (~3.7V) down to 2.8V, which is supplied to the AD5940 and CYW20736S. Inductive charging is initiated when the CWS-Stat is placed on a transmitter pad (Figure 3.2C). Charging is regulated by the wireless recharging IC, which features over-discharge protection and constant current / constant voltage charging capability to quickly charge the battery without overcharging.

3.2.3 CWS-Stat Operation

Electrochemical AFE Configuration

One of the major features of the CWS-Stat is its capability to perform a range of electrochemical sensing techniques – amperometry, square wave voltammetry, and potentiometry. This is achieved through the high reconfigurability of the electrochemical AFE. Figure 3.3 depicts the circuit configurations split between controlled potential techniques (amperometry / square wave voltammetry) and potentiometry. The primary differences between these is the configuration of the input TIA/BUF amplifier and the signal filtering used.

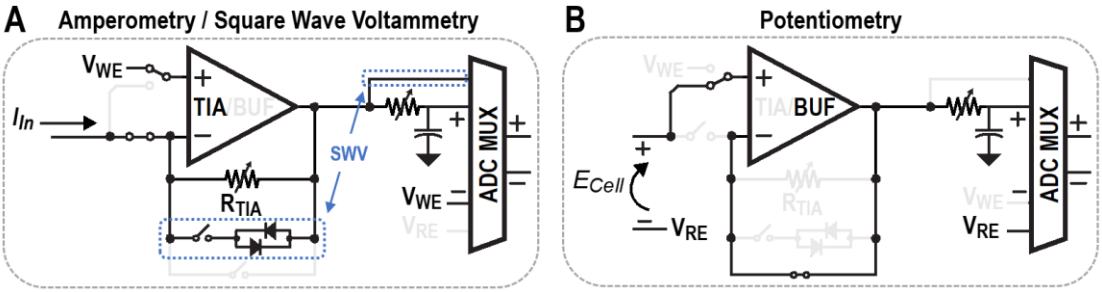

Figure 3.3. Electrochemical AFE configuration for (**A**) amperometry and square wave voltammetry (controlled potential techniques) [sections boxed in blue are used only for square wave voltammetry] and (**B**) potentiometry.

The TIA/BUF amplifier is configured as a transimpedance amplifier for controlled potential techniques, with the inverting input connected to the working electrode and the non-inverting input connected to V_{WE} (Figure 3.3A). In this configuration, the TIA converts input current I_{In} into a voltage to be measured by the ADC. The potential difference ($V_{WE} - V_{RE}$), set by the DAC, is applied to a connected electrochemical cell through the control amplifier and TIA. The operational range for the applied potential is +/- 1.0V with a resolution of 0.537mV (12-bit DAC, $V_{Ref} = 2.2V$). For square wave voltammetry, the diode pair is also connected to the amplifier's feedback path to support high inrush currents while using large R_{TIA} values. The ADC is configured to measure the differential voltage between the amplifier output and V_{WE} via the ADC MUX.

For potentiometry, the amplifier is configured as a voltage buffer (Figure 3.3B), whereby the working electrode is connected to the non-inverting input (and disconnected from the inverting input) and the unity feedback switch is closed. In this configuration, the amplifier buffers the input potential E_{Cell} to be measured by the ADC. The ADC is configured to measure the voltage between the amplifier output and V_{RE}.

Signal filtering on the AFE, which is used to suppress random electronic noise and electrochemical noise, is accomplished in both the analog and digital domains. A single pole low pass analog filter is formed by a programmable resistor and a 1µF capacitor located at the output of the TIA/BUF amplifier. The resistor is set to 20kΩ for amperometry, resulting in a 3dB cutoff frequency of 7.96 Hz, and set to 1MΩ for potentiometry for a cutoff frequency of 0.159 Hz. A wider bandwidth is used for amperometry to prevent the filter's settling time from causing measurement inaccuracies of the capacitive currents found in amperometry tests. The RC filter is bypassed altogether for square wave voltammetry for the same reason. The ADC output connects to a digital $sinc^3$ filter cascaded by a $sinc^2$ filter. For both amperometry and potentiometry, the oversampling ratios of the $sinc^3$ and $sinc^2$ filters are set to 5 and 1333, respectively (the maximum setting on the AFE), producing an overall filter 3dB bandwidth of 38.32 Hz (sampling rate = 800 kSPS). Digital filtering for square wave voltammetry is chosen such that the sampling integration time (i.e. the conversion time / total time for the ADC and digital filters to produce a measurement) falls within the last 20% of the square wave's pulse duration. Integration times for various oversampling ratios (OSR) and applicable frequencies for these integration times are listed in Table 3.1. Note that the frequency response of digital *sinc* filters is similar to that of averaging / integration methods commonly used in electrochemical analysis. Additionally, a 60 Hz / 50 Hz power line interference filter is used for amperometry and potentiometry tests, though not for square wave voltammetry due to the filter's long conversion time.

Table 3.1. Integration Time Thresholds for Square Wave Voltammetry

Integration Time [ms]	Max Applicable f_{SWV}* [Hz]	Sampling Rate [kSPS]	$\mathbf{sinc^3}$ OSR	$\mathbf{sinc^2}$ OSR	3dB BW [Hz] **
16.68	11	800	5	1333	38.32
13.36	14	800	5	1067	48.25
11.13	17	800	5	889	54.57
10.02	19	800	5	800	63.89
8.36	23	800	5	667	77.03

*Excitation frequency for square wave voltammetry
**Found from simulation

In addition to being filtered, the signals produced during controlled potential tests are amplified by the TIA and PGA to ensure that their levels are always within the detectable limits of the ADC over a wide range of input current. For amperometry, the user has the option to use an autoranging system which automatically adjusts the TIA and PGA gains during tests to engage the correct gain values given any signal level (see Supplementary Material 3.6.2).

BLE Device Control

All control of the CWS-Stat is done wirelessly over BLE as depicted in Figure 3.4. The CWS-Stat is configured as a Bluetooth Generic Attribute Profile (GATT) server and hosts custom services and characteristics which a GATT client (e.g. a smartphone) can interact with. The BLE GATT is organized into "services" which group together pieces of data referred to as "characteristics." Each electrochemical technique available on the CWS-Stat – amperometry, square wave voltammetry, and potentiometry – has two services: a configuration service and a measurement data service. The configuration services contain characteristics for setting test parameters (e.g. applied potential for chronoamperometry, excitation frequency for square wave voltammetry, and test duration for potentiometry). The measurement data services act as unique data channels for transmitting data, and each trivially contains a characteristic for measurement data. Prior to transmission, measurement data acquired through the ADC is converted to relevant measurement units – current in pA for amperometry and square wave voltammetry, and potential in μV for potentiometry. A complete list of all BLE services and characteristics found on the CWS-Stat GATT server is provided in Supplementary Material 3.6.3.

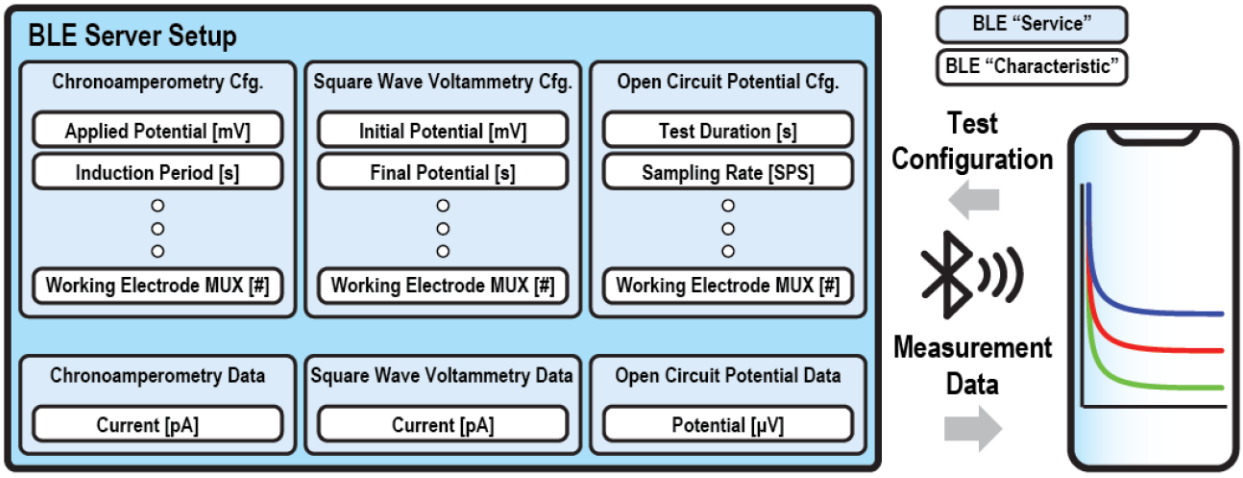

Figure 3.4. BLE operation for the CWS-Stat. The BLE GATT server contains BLE services for configuring electrochemical tests and services for test measurement data. All operation is controlled by a BLE GATT client such as a smartphone.

The sequence for running electrochemical tests with a mobile device is as follows: 1) the mobile device sets all the test parameters through the configuration services, 2) the mobile device sends a "Start" signal to the CWS-Stat to commence testing, 3) measurement data is transmitted to the mobile device through the data services via BLE "notifications" or "indications," 4) the CWS-Stat sends a "Finished" signal to the mobile device to indicate that testing has completed. Throughout this entire sequence, the user can visually verify that the CWS-Stat is operating correctly through an LED status indicator found on the CWS-Stat's PCB. When idling (no measurements being taken), the LED will flash green every 2 seconds, and during measurements the device will flash blue. These LED color sequences, in addition to sequences for other device operations (e.g. OTA updates or wireless recharging) are listed in Supplementary Material 3.6.4.

3.2.4 Electrochemical Method Testing

The following tests were performed to characterize the electrochemical sensing performance of the CWS-Stat in terms of accuracy relative to a commercial potentiostat. All tests were conducted at room temperature.

Chronoamperometry: Detection of H_2O_2 in PBS of pH 7.4 at an applied potential of +0.6V v. Ag/AgCl. The working and counter electrode were made of platinum (Pt).

Square Wave Voltammetry: Detection of L-Dopa in PB with an applied potential scan of -0.3V to 0.7V v. Ag/AgCl with 2mV steps, excitation frequency of 20Hz, and square wave amplitude of 50mV. The working electrode was a hollow microneedle electrode made of an acrylate-based polymer and packed with carbon paste (65% graphite powder and 35% mineral oil in weight). The counter electrode material was Pt.

Potentiometry: Detection of sodium in NaCl using an ion-selective electrode. The electrode had been pre-conditioned in NaCl aqueous solution (100 mM) for 30 minutes. OCP responses were measured versus Ag/AgCl.

Additionally, an open-circuit test (in which the working electrode input is left floating) was conducted across multiple transimpedance gain values to evaluate the noise performance of the CWS-Stat for current measurement tests and to find its absolute limit of the detection (i.e. minimum detectable signal).

3.2.5 Power Optimizations

Both the AD5940 AFE and CYW20736S BLE module feature configurable "sleep" modes to reduce average power consumption by power-gating and/or clock-gating circuit blocks. This is leveraged on the AFE by turning the ADC and digital filters *on* solely for periodic sampling events and turning them *off* outside of these events. Furthermore, the microcontroller and BLE radio on the CYW20736S are deterministically gated between sampling events. Note that throughout an entire electrochemical test, the DAC, control amplifier, and TIA/BUF amplifier are left on to maintain the reference electrode potential and maintain / measure the working electrode potential for potential-controlled / potentiometry tests.

3.3 Results & Discussion

3.3.1 Electrochemical Sensing Performance

Electrochemical Methods

All electrochemical method responses from the CWS-Stat for amperometry, square wave voltammetry, and potentiometry are plotted in Figure 3.5 and superimposed with responses from a commercial potentiostat (EmStat3, PalmSens BV, Utrecht, Netherlands). Amperometry steady state currents of 4.28, 8.49, amd 12.34 µA were observed for the CWS-Stat versus 4.25, 7.9, and 11.3 µA for the commercial potentiostat, giving the CWS-Stat errors of 0.55, 7.43, and 9.22% for each concentration. For square wave voltammetry, the CWS-Stat measured peak currents of 7.36, 11.66, and 14.12 µA versus 7.91, 11.66, and 14.12 µA producing errors of 6.99, 0.32, and 0.33%. For potentiometry, the CWS-Stat measured potentials of 0.2065, 0.2144, 0.2204, 0.2248, and 0.2285V versus 0.1948, 0.2017, 0.2055, 0.2088, and 0.2115V, producing errors of 6.01, 6.30, 7.22, 7.66, and 8.06%.

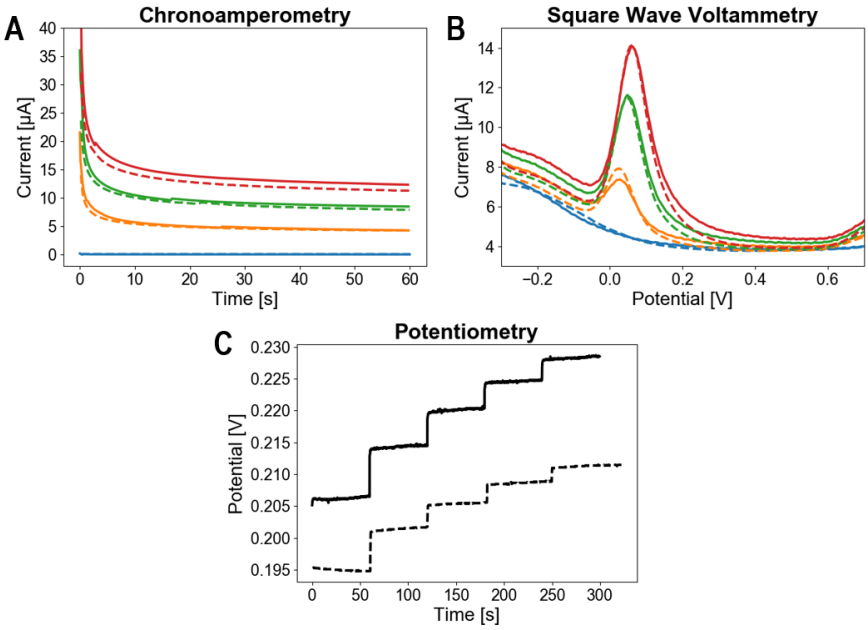

Figure 3.5. Electrochemical method comparison between the CWS-Stat and commercial potentiostat (solid: CWS-Stat, dashed: commercial potentiostat) for (**A**) amperometric detection of H_2O_2 in PBS (+5, +10, +15 µM), (**B**) square wave voltammetric detection of L-Dopa in PB (+5, +10, +15 µM), and (**C**) potentiometric detection of sodium (+100, +150 +200, +250, +300 mM).

Noise Performance & Limit of Detection

Figure 3.6 depicts the input-referred noise levels from the open-circuit test for gain values of 36kΩ to 90MΩ. It was observed that ADC quantization noise dominated for gain values less than 10MΩ, and other electronic noise (e.g. thermal and flicker noise) dominated for 10MΩ and above. The lowest input referred noise level was found to be σ = 1.2pA (gain = 90MΩ), giving the CWS-Stat a limit of detection (LOD) of 3*σ = 3.6pA.

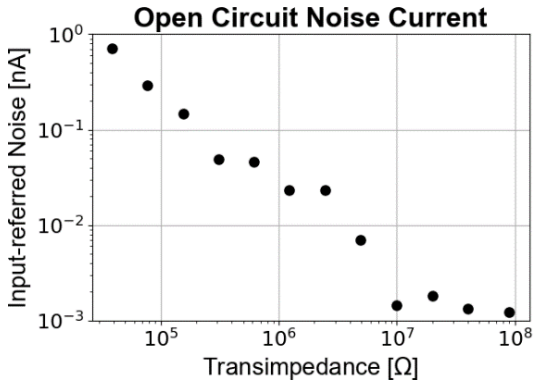

Figure 3.6. Input-referred referred noise for amperometry. Noise levels were calculated as the standard deviation of measured electrical current from a 60s open-circuit test (sampling interval = 0.1s). Noise is plotted for transimpedance gain values (set by the TIA feedback resistor and PGA) for 36kΩ – 90MΩ.

3.3.2 Power Consumption

Current consumption of the CWS-Stat was measured with a benchtop oscilloscope (PicoScope 5444B, Pico Technology, Cambridgeshire, UK) to verify placement of the AD5940 and CYW20736S into low power sleep modes and to find the device's operational battery life (Figure 3.7).

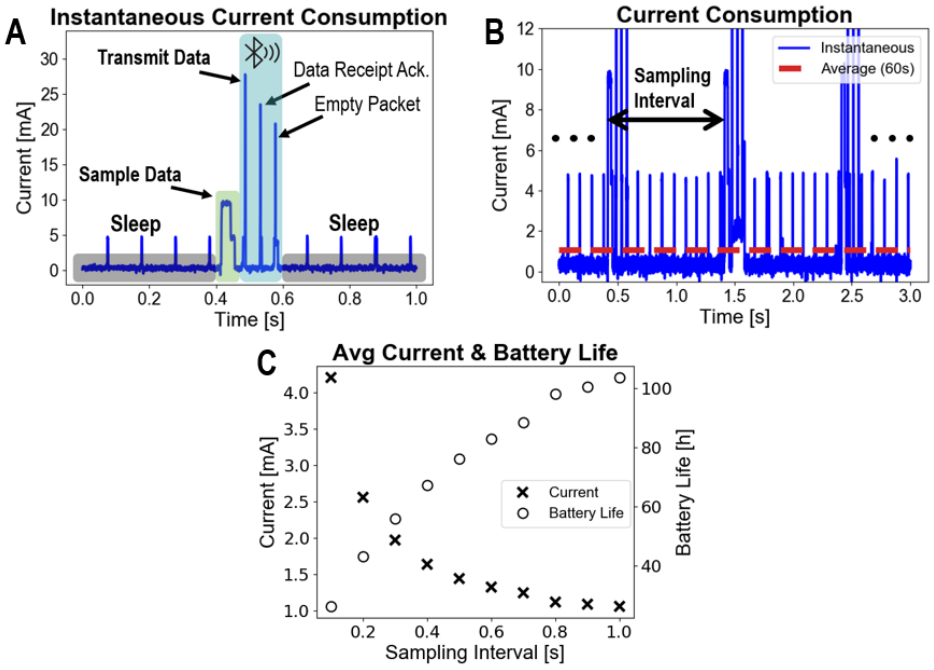

Figure 3.7. Current consumption of the CWS-Stat in amperometry mode. (**A**) Instantaneous current consumption for 1 sampling event. (**B**) Instantaneous and average current consumption for a 60s test (sampling interval of 1s) zoomed into the first 3 sampling events. (**C**) Average current and battery life for continuous sampling at intervals of 0.1s – 1s (sampling rate of 10Hz – 1Hz) in 0.1s steps.

Figure 3.7A depicts the instantaneous current consumption before, during, and after a single sampling event. An increase in current to ~10mA is observed at t = 0.4s, indicating that the microcontroller, ADC, and digital filters have been turned on to begin a sampling event. The current drops down shortly after, indicating that data had been sampled and the microcontroller, ADC, and digital filters have turned off. Next, the current spikes to ~20-30mA, indicating that the BLE radio and microcontroller have turned on, which occurs for 3 sequential BLE connection events. During the first, data is transmitted to a mobile device. Next, the CWS-Stat receives a confirmation from the mobile device that the measurement data had been properly received. Lastly, the CWS-stat receives an empty BLE packet from the mobile device, telling the CWS-Stat that no further BLE communication will take place, allowing the BLE radio to be kept off until the next sampling event. Before and after these events, the low current levels labeled “Sleep” verify that ICs were successfully placed into low power modes. Small spikes of ~5mA appear every 100ms – this is the CYW20736S periodically waking up to briefly to

perform basic system operations, such as flashing the CWS-Stat's LED, taking battery level measurements, or checking if data needs to be retransmitted due to a BLE disconnect.

Figure 3.7B depicts the average current consumption of a 60s amperometry test (sampling interval = 1s) and the instantaneous current of 3 sampling events during this test for reference. Notice that the average current lies close to the "Sleep" current found between sampling events, as the CWS-Stat remains primarily in sleep mode given the long sampling interval**.** Figure 3.7C depicts the average current consumption and consequent battery life when sampling at shorter sampling intervals. At a sampling interval of 0.1s, the ADC, digital filters, microcontroller, and BLE radio are on more frequently, raising the average consumption to 4.20mA, resulting in a battery life of 1 day and 2.2 hours. Current consumption decays back to 1.06mA as the sampling interval is increased back to 1s, resulting in a battery life of 4 days and 7.6 hours.

Additionally, the CWS-Stat can be placed into an ultra-low power mode via a BLE command whereby all components are turned off for a preset duration of time. In this mode, the CWS-Stat consumes 53.5µA. Duty cycling this ultra-low power mode with continuous sampling allows for significant battery life gains. For instance, 10% duty cycling with 1 minute of continuous sampling mode (sampling interval = 1s) followed by 9 minutes of ultra-low power mode results in average current consumption of 154µA and a battery life of approximately 30 days.

3.3.3 Comparison to Similar Works

Table 3.2 summarizes this work's capabilities and performance and compares them to state-of-the-art potentiostats found in literature. Owing to the low number of active components (each with low quiescent current consumption) and power optimizations implemented, this work demonstrates the lowest current consumption compared to previous arts. It is the only device capable of performing both potentiometry and controlled potential techniques on any of its 4 multiplexed inputs, and the only device designed for wearable applications which can perform a voltammetric technique. Lastly, it is the only work capable of wireless recharging

Table 3.2. Comparison of State-of-the-Art Potentiostats

	[39]	[40]	[41]	[42]	[43]	[44]	[32]	[30]	[31]	[36]	**This Work**
Year	2011	2015	2018	2019	2020	2016	2015	2015	2016	2020	**2021**
Potential Range	+/- 0.99	+/- 1.5V	+/- 1.5V	+/- 1.2 V	+/- 0.792 V	-0.2V to 0.3V (Lactoferrin), 0.5V (Glucose)	-0.3 V (Uric Acid)	-0.1 V (Lactate)	0 V (Glucose & Lactate)	+/- 1.2 V	**+/- 1.0V**
Current Range	100nA to 50uA	-	180µA	100uA	-	1nA to 200µA	-	-	1nA to 2.8 µA	-	**10nA to 2mA**
LOD *	-	600fA	90nA	91nA	4.5nA	648pA	-	-	-	-	**3.6pA**
Current Consumption **	-	-	4.8mA	20 mA	11mA	13.38 mA	7 mA	5mA	-	15 mA	**1.06 mA**
PCB Area [cm^2]	92.40	64.00	-	5.40	4.38	6.44	3.42	-	-	-	**5.31**
Rechargeability	-	-	Yes, wired	-	-	-	-	-	-	Yes, wired	**Yes, Wireless**
Battery Type	-	-	Li-poly 3.7V 240mAh	-	-	-	2x Silver Oxide 1.55V 33mAh	Li-ion 3.0V	Li-poly 3.7V 105mAh	Li-poly 3.7V 150mAh	**Li-poly 3.7V 110mAh**
Communication	USB	USB	BLE	USB	USB	Smartphone Integration	BLE	BLE	Bluetooth	BLE	**BLE**
ADC Resolution	12-Bit	24-Bit	10-Bit	15-Bit	12-Bit	16-Bit	12-Bit	12-Bit	10-Bit	16-Bit	**16-Bit**
DAC Resolution	12-Bit	16-Bit	16-Bit	12-Bit	10-Bit	14-Bit	-	-	-	-	**12-Bit**
Multichannel Capability	N	N	N	N	N	Y - 2 Inputs (CA, EIS, or POT on any)	N	Y - 2 Inputs (1 CA, 1 ECG)	Y - 4 Inputs (2 CA, 2 POT)	Y - 13 Inputs (12 CA/CV, 1 POT)	**Y - 4 Inputs (CA, POT, or SWV on any)**
Multimodal Capability	CV, LSV, SWV	CV, DPV, POT	CA, CV, DPV, POT, SWV	ASV, CA, CV, LSV, SWV	CA, CV, NPV, SWV	CA, EIS, POT	CA	CA, ECG	CA, POT	CA, CV, POT	**CA, POT, SWV**
Application	Open-source, Portable	Open-source, Portable	Open-source, Portable	Open-source, Portable	Open-source, Portable	Point-of-care (POC)	Wearable Sensing	Wearable Sensing	Wearable Sensing	Wearable Sensing	**Wearable Sensing**

* Limit of detection calculated from 3x input referred noise if LOD not reported
** For continuous sensing; calculated from power consumption if current consumption not reported

ASV: Anodic Stripping Voltammetry; CA: Chronoamperometry; CV: Cyclic Voltammetry; DPV: Differential Pulse Voltammetry; ECG: Electrocardiogram; EIS: Electrochemical Impedance Spectroscopy; LSV: Linear Sweep Voltammetry; NPV: Normal Pulse Voltammetry; POT: Potentiometry

3.4. Wearable Electrochemical Sensor Integration

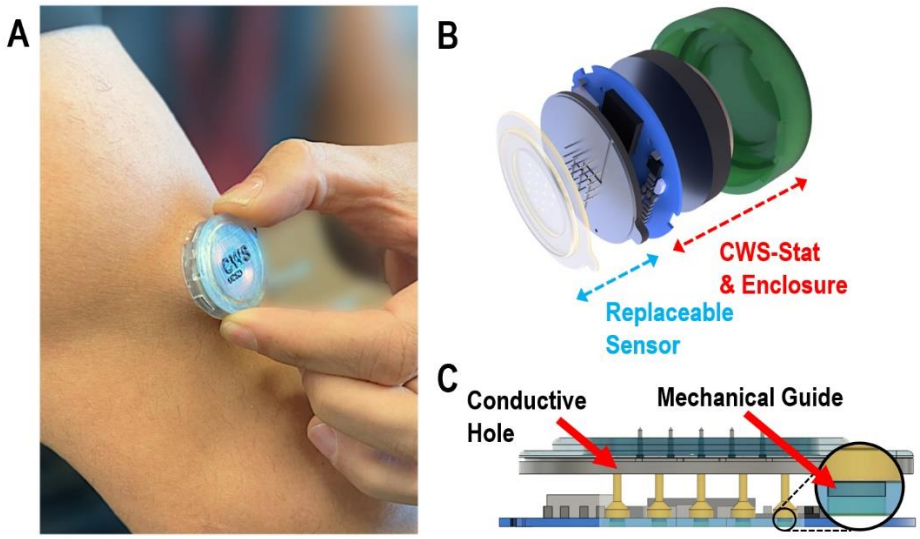

Figure 3.8. Integration of the CWS-Stat into wearable microneedle-based biosensing system. (**A**) Sensor patch applied to the subject's arm for on-body trial. (**B**) Exploded view (rendered) of the wearable patch consisting of microneedle sensor, CWS-Stat (assembled PCB, battery, wireless charging coil), and device enclosure. (**C**) Depiction of the CWS-Stat sensor interface. Pins insert into conductive holes on the microneedle sensor made from sputter deposited metal into CNC milled holes. The mechanical guides on the pins provide mechanical retention to the CWS-Stat PCB.

The CWS-Stat was fully integrated with a microneedle-based electrochemical biosensor to form a wearable biosensing system to measure biomarkers from the user's interstitial fluid (ISF) (Figure 3.8). The CWS-Stat and microneedle sensor are housed within a 3D-printed plastic enclosure, which offers liquid and damage protection without significantly degrading RF performance. The gold-plated pins on the CWS-Stat are inserted into electrically conductive holes on the underside of the microneedle sensor (Figure 3.8C), connecting the biosensor to the AFE's multiplexed inputs. The mechanical retention of the electrode pins to the CWS-Stat allows for a robust interface between the CWS-Stat and microneedle sensor after multiple sensor removals / replacements.

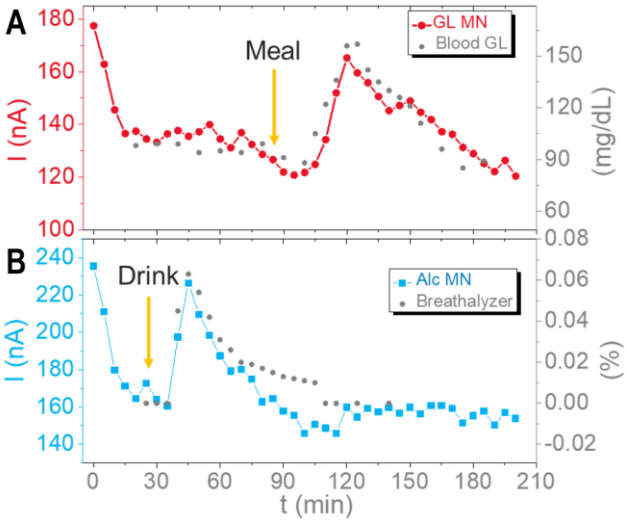

Figure 3.9. On-body results of the microneedle-based electrochemical biosensing system. (**A**) Microneedle system ISF glucose results compared to commercial glucose meter test strip. (**B**) Microneedle system ISF alcohol results compared to commercial breathalyzer.

The system was tested on-body for multiplexed amperometric sensing of glucose and alcohol (Figure 3.9). Glucose results show good correlation between the microneedle system and blood glucose, with the ISF measurements tracking blood glucose levels before and after the subject consumed a meal. Alcohol measurements show simultaneous peaks in the ISF alcohol and breathalyzer measurements from 3 glasses of wine, though the tracking before and after this peak is not as evident as that found with glucose. Since breathalyzer results are only an estimate of blood alcohol, it is not clear whether the tracking is lost due to the microneedle biosensor or the breathalyzer accuracy.

3.5. Conclusion

This paper has presented the design of a wireless, reconfigurable potentiostat for wearable electrochemical biosensing applications. It can perform amperometry, square wave voltammetry, and potentiometry tests on any of its four multiplexed inputs. It features multiple current ranges of +/-2.15mA down to +/-16.2nA with an absolute limit of detection 3.6pA. All communication with the device is handled over Bluetooth Low Energy (BLE), including test configuration and measurement data transmission. Its power optimizations allow it to support nearly 30 days of continuous sensing

(amperometry) with a 110mAh battery. Additionally, it features wireless charging capability, removing the need to replace the battery after its depletion. Its performance and capabilities are validated by the CWS-Stat's successful integration into a wearable microneedle-based biosensing system. Overall, its compact size, multi-technique capability, wireless operation, and long battery life make the CWS-Stat a versatile electrochemical sensing platform to support the continual advancement of wearable electrochemical biosensing systems.

3.6. Supplementary Material

3.6.1 Programming of CWS-Stat

Figure S3.1 depicts the programming and reprogramming procedure for the CWS-Stat. Initial programming the electronics is accomplished using Cypress' WICED SMART, a software development kit (SDK) which provides an Eclipse-based integrated development environment (IDE) for building firmware and downloading it to the electronics. Programming uses UART connections (Tx, Rx, VCC, GND), and requires a physical connection between the electronics and a personal computer which hosts the firmware. This is accomplished by first connecting the electronics to a Cypress BCM92073X_LE_KIT development kit through a 6-pin Molex PicoBlade cable, and connecting the kit to the personal computer using a micro-USB cable. The development kit is needed specifically for its on-board FTDI USB-UART interface chip, which converts serial UART signals into serial USB signals. Thereafter, the programming header of the electronics (which has no active components) is snapped or cut off, making the CWS-Stat ready to be integrated into electrochemical biosensing systems. Reprogramming can be done through over-the-air (OTA) updates via BLE.

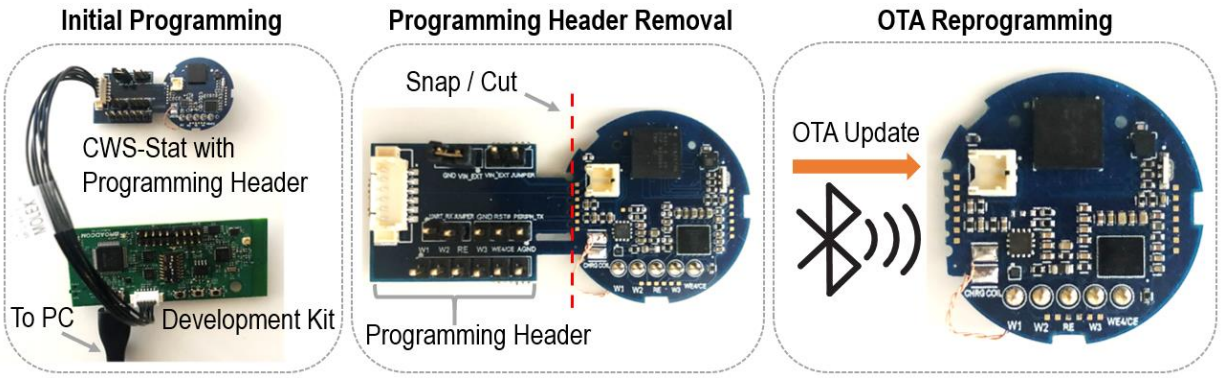

Figure S3.1. Programming and reprogramming steps of the CWS-Stat, including initial programming from a PC hosting the firmware, removal of the programming header, and OTA reprogramming through wireless BLE communication

3.6.2. Autoranging System

The autoranging system is used to automatically set the transimpedance gain of the CWS-Stat during amperometric measurements to prevent ADC saturation. The algorithm, depicted in Figure S3.2A, recursively tests different transimpedance levels until the signal level is within 20% to 80% of the ADC's full range. Each gain level covers 12.04dB of range, except for the highest transimpedance level (upper left bar in Figure S3.2B) which covers 73.1dB from 16.2nA down to 3.6pA (the limit of detection for the CWS-Stat), and the lowest transimpedance gain level (lower right bar in Figure S3.2B) which extends from 0.83mA up to 2.15mA for a range of 8.3dB. The autoranging system therefore supports the CWS-Stat's full range of 3.6pA to 2.15mA, or 175.5dB.

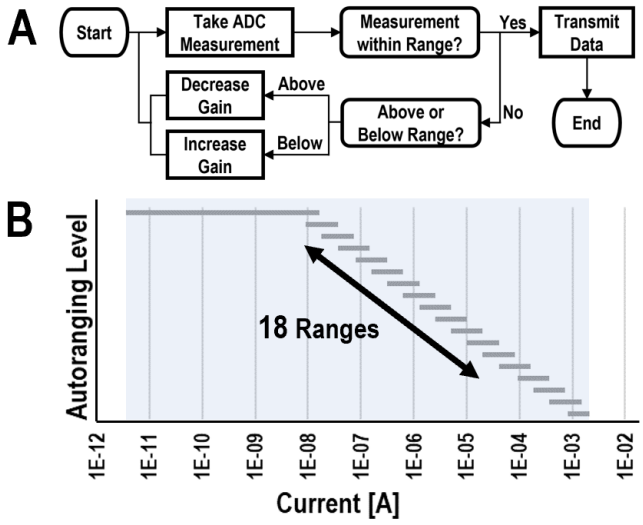

Figure S3.2. Autoranging system for amperometric measurements. (**A**) Flowchart of autoranging algorithm. (**B**) Input current ranges for each of the 17 levels available to the autoranging system.

3.6.3. CWS-Stat BLE GATT API

Device Info Service

Manufacturer

- Properties: Read
- Type: UTF-8 String
- Description: Manufacturer of device

Model Number

- Properties: Read
- Type: UTF-8 String
- Description: Model number of device

System ID

- Properties: Read
- Type: UTF-8 String
- Description: System ID of device

Firmware Revision

- Properties: Read
- Type: UTF-8 String
- Description: Firmware revision of device

Battery Service

Battery Level

- Properties: Read
- Type: UINT8
- Description: Battery level percentage

Power Service

System Power

- Properties: Write No Response
- Type: UINT8
- Description: Writing a 1 to this characteristic will turn device off (deep sleep). Device will only power on if placed on charger.

Sensing Configuration Service

Mode Select

- Properties: Read/Write
- Type: UINT8
- Description: Changes the operational mode of the device by writing the following values to the characteristic:
  - 0 - Amperometry Mode
  - 1 - Potentiometry Mode
  - 3 - Square Wave Voltammetry Mode
  - 4 - Delay Mode

Start/Stop Sensing

- Properties: Read/Write
- Type: UINT8
- Description: Function depends on the operational mode set by the *Mode Select* characteristic:
  - For *Amperometry Mode, Potentiometry Mode,* and *Square Wave Voltammetry Mode,* writing a 1 to this characteristic will start the electrochemical test. Writing a 0 will stop the test.
  - For *Delay Mode, Delay Configuration Service: Ultra Low Power* Mode is enabled, writing a 1 to this characteristic will place the device into ultra low power mode. The device will be unresponsive until the device wakes up from the timed ultra low power mode.

Sensing Complete

- Properties: Read/Notify
- Type: UINT8
- Description: This characteristic will have a value of 0 during tests, and 1 when no tests are running for *Amperometry Mode, Potentiometry Mode,* and *Square Wave Voltammetry Mode.* Upon any test completion, the device will send a notification with the value 1 to a connected peer, indicating that the device has completed a test and is ready to start another.

Amperometry Data Service

Data - Current

- Properties: Read/Notify

- Type: INT32
- Description: This is the measurement data channel for *Amperometry Mode*. The device will send notifications or indications containing measurement data in units of pico-amps (pA).

Square Wave Voltammetry Data Service

Data - Current

- Properties: Read/Notify
- Type: INT32
- Description: This is the measurement data channel for *Square Wave Voltammetry Mode*. The device will send notifications or indications containing measurement data in units of pico-amps (pA).

Potentiometric Data Service

Data - Potential

- Properties: Read/Notify
- Type: INT32
- Description: This is the measurement data channel for *Potentiometry Mode*. The device will send notifications or indications containing measurement data in units of micro-volts (uV).

Amperometry Configuration Service

Electrode Selection

- Properties: Read/Write
- Type: UINT8
- Description: Bitmask for selecting the working electrode (WE) and counter electrode (CE) for current-measurement tests, according to the following:
  - Bits [3-0] – WE selection. Set any of the following bits to 1 to enable any of the electrodes (Ex) as a working electrode.
    - Bit 0: E1
    - Bit 1: E2
    - Bit 2: E3
    - Bit 3: E4
  - Bits [7-4] – CE selection. Set any of the following bits to 1 to enable any of the electrodes (Ex) as a counter electrode.
    - Bit 4: E1
    - Bit 5: E2
    - Bit 6: E3
    - Bit 7: E4
  - Note 1: Any number of working electrodes or counter can be selected.
  - Note 2: Setting Bits [7-4] to 0 sets the device to operate in a 2-electrode configuration, in which the counter electrode is internally shorted to the reference electrode.
  - Example 1: Bitmask = 1000 0001 sets WE = E1, CE = E4 (3-electrode configuration)
  - Example 2: Bitmask = 1000 1100 sets WE = E3,E4, CE = E4 (3-electrode configuration)
  - Example 3: Bitmask = 0000 0010 sets WE = E2 (2-electrode configuration)

Induction Period Duration

- Properties: Read/Write
- Type: UINT16
- Description: This is the amount of time to apply 0V to the electrochemical cell prior to stepping the potential to *Applied Potential*. Measurement data is acquired during this period.
  - Units: ms
  - Range: 0 to 65535

Applied Potential

- Properties: Read/Write
- Type: INT16
- Description: Constant potential to apply to an electrochemical cell upon completion of the induction period
  - Units: mV
  - Range: -1000 to +1000

Sample Count

- Properties: Read/Write
- Type: UINT16
- Description: Number of samples to take for an electrochemical test
  - Note: a 0th data point is collected at time t = 0, independent of what is entered for sample count. Thus, the total test time is: (*Sample Interval*) * (*Sample Count*).
  - Range: 0 to 65535

Sampling Interval

- Properties: Read/Write

- Type: UINT16
- Description: Time period between measurements (e.g. if sample period = 500ms, two samples will occur a second)
  - Units: ms
  - Range: 0 to 65535

Gain Level

- Properties: Read/Write
- Type: UINT8
- Description: If value is set to 0, autoranging is enabled for current-measurement tests. Else, this value sets the I-to-V gain according to *Table S3.1. Gain Table*, with autoranging off.

Potentiometry Configuration Service

Electrode Selection

- Properties: Read/Write
- Type: UINT8
- Description: Bitmask for selecting the working electrode (WE) potential-measurement tests, according to the following:
  - Bits [3-0] – WE selection. Set any of the following bits to 1 to enable any of the electrodes (Ex) as a working electrode.
    - Bit 0: E1
    - Bit 1: E2
    - Bit 2: E3
    - Bit 3: E4
  - Note: Any number of working electrodes or counter can be selected
  - Example: Bitmask = 0001 sets WE = E1

Sample Count

- Properties: Read/Write
- Type: UINT16
- Description: Number of samples to take for an electrochemical test.
  - Note: a 0th data point is collected at time t = 0, independent of what is entered for sample count. Thus, the total test time is: (*Sample Interval*) * (*Sample Count*)
  - Range: 0 to 65535

Sampling Interval

- Properties: Read/Write
- Type: UINT16
- Description: Time period between measurements (e.g. if sample period = 500ms, two samples will occur a second)
  - Units: ms
  - Range: 0 to 65535

Square Wave Configuration Service

Electrode Selection

- Properties: Read/Write
- Type: UINT8
- Description: See *Amperometry Configuration Service: Electrode Selection*

Induction Period Duration

- Properties: Read/Write
- Type: UINT16
- Description: Amount of time to apply *Ramp Initial Potential* prior to initiating the square wave sequence. No data is collected during this period.
  - Units: ms
  - Range: 0 to 65535

Ramp Number of Steps

- Properties: Read/Write
- Type: UINT8
- Description: This is the number of potential steps to take while ramping from *Ramp Initial Potential* to *Ramp Final Potential*. The potential difference for each step is (*Ramp Final Potential – Ramp Initial Potential*) / (*Ramp Number of Steps*)
  - Range: 0 to 255

Ramp Initial Potential

- Properties: Read/Write
- Type: INT16
- Description: Initial potential to apply to the electrochemical cell for potential ramp
  - Units: mV
  - Range: -1000 to +1000

Ramp Final Potential

- Properties: Read/Write
- Type: INT16
- Description: Final potential to apply to the electrochemical cell for potential ramp
  - Units: mV
  - Range: -1000 to +1000

Square Wave Excitation Frequency

- Properties: Read/Write
- Type: UInt8
- Description: Excitation frequency of the applied square wave
  - Units: Hz
  - Range: 1 to 20

Square Wave Amplitude

- Properties: Read/Write
- Type: UINT16
- Description: Amplitude of applied square wave (distance from mean value, not peak-to-peak)
  - Units: mV
  - Range: 0 to 50

Gain Level

- Properties: Read/Write
- Type: UINT8
- Description: This value sets the I-to-V gain according to *Table S3.1. Gain Table*

Delay Configuration Service

Ultra Low Power (ULP) Enable

- Properties: Read/Write
- Type: UINT8
- Description: Enables / disables ultra low power mode during a delay according to:
  - 0: Disabled
  - 1: Enabled

Delay Duration

- Properties: Read/Write
- Type: UINT16
- Description: Time spent during delay
  - Units: seconds (s)
  - Range: 0 to 65535

Table S3.1. Gain Table

Gain Level	R_{TIA} [I/V]	$A_{V,PGA}$ [V/V]	Transimpedance Gain ($R_{TIA} * A_{V,PGA}$) [I/V]
1	110	4	440
2	110	9	990
3	1000	2	2000
4	1000	4	4000
5	1000	9	9000
6	2000	9	18000
7	4000	9	36000
8	8000	9	72000
9	16000	9	144000
10	32000	9	288000
11	64000	9	576000
12	128000	9	1152000
13	256000	9	2304000
14	512000	9	4608000
15	10000000	1	10000000
16	10000000	2	20000000
17	10000000	4	40000000
18	10000000	9	90000000

3.6.4. LED Status Indicator

The LED on the CWS-Stat is programmed to flash different colors and sequences to inform the user of its current state according to Table S3.2.

Table S3.2. LED Status Indicator Key

LED Color Sequence	Operating Mode
Blue / Red Alternating	Bluetooth Pairing
Yellow, Solid	Calibration
Green, Blinking	Idle (Paired)
Green / Red Alternating	Idle, Low Battery (Paired)
Blue, Blinking	Sensor Measurement (Paired)
Magenta, Blinking	OTA Update
Green, Fade-in Fade-out	Charging Battery

Chapter 4 Conclusion

Low-power electronics are a crucial element of wearable electrochemical biosensing systems. Design of these electronics requires knowledge in areas such as integrated circuits, PCB fabrication technologies, antenna design, battery technologies, sensor interfaces, and wireless communication technologies. This thesis attempts to provide an overview of these and present a design which utilizes them.

The realized electronics presented in this work is a compact, low-power, wireless electronic platform for wearable electrochemical biosensing applications. The utility of the design is its capability of multiplexed sensing from a variety of electrochemical biosensors due to its multichannel inputs and high level of reconfigurability. This enables multi-analyte sensing from biological fluids such as sweat, saliva, and interstitial fluid, providing wearers insight into their physiology to monitor their health / fitness.

Overall, this work underscores the proximity that wearable electrochemical biosensing devices are to becoming popularized in the wearable devices space like their physical and electrical-based biosensing counterparts (e.g. motion sensing and ECG recording devices). Given the potential of these electrochemical sensing systems to provide a more comprehensive view of health or fitness compared to other biosensing techniques, it is only a matter of time before the technology is adopted everywhere.

References

[1] J. Kim, A. S. Campbell, B. E. F. de Ávila, and J. Wang, "Wearable biosensors for healthcare monitoring," *Nature Biotechnology*, vol. 37, no. 4. 2019, doi: 10.1038/s41587-019-0045-y.

[2] G. Aroganam, N. Manivannan, and D. Harrison, "Review on Wearable Technology Sensors Used in Consumer Sport Applications," *Sensors (Basel, Switzerland)*, vol. 19, no. 9. 2019, doi: 10.3390/s19091983.

[3] M. P. Turakhia, M. Desai, H. Hedlin, A. Rajmane, N. Talati, T. Ferris, S. Desai, D. Nag, M. Patel, P. Kowey, J. S. Rumsfeld, A. M. Russo, M. T. Hills, C. B. Granger, K. W. Mahaffey, and M. v. Perez, "Rationale and design of a large-scale, app-based study to identify cardiac arrhythmias using a smartwatch: The Apple Heart Study," *American Heart Journal*, vol. 207, 2019, doi: 10.1016/j.ahj.2018.09.002.

[4] J. Wang, "Electrochemical glucose biosensors," *Chemical Reviews*, vol. 108, no. 2. 2008, doi: 10.1021/cr068123a.

[5] B. Schazmann, D. Morris, C. Slater, S. Beirne, C. Fay, R. Reuveny, N. Moyna, and D. Diamond, "A wearable electrochemical sensor for the real-time measurement of sweat sodium concentration," *Analytical Methods*, vol. 2, no. 4, 2010, doi: 10.1039/b9ay00184k.

[6] W. Jia, A. J. Bandodkar, G. Valdés-Ramírez, J. R. Windmiller, Z. Yang, J. Ramírez, G. Chan, and J. Wang, "Electrochemical tattoo biosensors for real-time noninvasive lactate monitoring in human perspiration," *Analytical Chemistry*, vol. 85, no. 14, 2013, doi: 10.1021/ac401573r.

[7] J. Kim, I. Jeerapan, S. Imani, T. N. Cho, A. Bandodkar, S. Cinti, P. P. Mercier, and J. Wang, "Noninvasive Alcohol Monitoring Using a Wearable Tattoo-Based Iontophoretic-Biosensing System," *ACS Sensors*, vol. 1, no. 8, 2016, doi: 10.1021/acssensors.6b00356.

[8] K. Y. Goud, C. Moonla, R. K. Mishra, C. Yu, R. Narayan, I. Litvan, and J. Wang, "Wearable Electrochemical Microneedle Sensor for Continuous Monitoring of Levodopa: Toward Parkinson Management," *ACS Sensors*, vol. 4, no. 8, 2019, doi: 10.1021/acssensors.9b01127.

[9] D. R. Seshadri, R. T. Li, J. E. Voos, J. R. Rowbottom, C. M. Alfes, C. A. Zorman, and C. K. Drummond, "Wearable sensors for monitoring the physiological and biochemical profile of the athlete," *npj Digital Medicine*, vol. 2, no. 1, 2019, doi: 10.1038/s41746-019-0150-9.

[10] Texas Instruments, "LMP91000: Configurable AFE Potentiostat for Low-Power Chemical Sensing Applications," 2011. [Online]. Available: www.ti.com.

[11] Analog Devices, "AD5940: High Precision, Impedance, and Electrochemical Front End," 2019. [Online]. Available: www.analog.com.

[12] Maxim Integrated, "MAX30131: Ultra-Low Power Programmable AFE for Electrochemical Sensors," 2019.

[13] Cypress Semiconductor Corp., "CYW20736: Single-Chip Bluetooth Low Energy System-On-Chip," 2014.

[14] Nordic Semiconductor, "nRF52832: Multiprotocol Bluetooth 5, ANT/ANT+ and 2.4 GHz proprietary System-on-Chip," 2017.

[15] ON Semiconductor, "RSL10: Bluetooth 5 Radio System-on-Chip (SoC)," 2018.

[16] Cypress Semiconductor Corp., "CYW20736S: Bluetooth Low Energy System-in-Package (SiP) Module," 2014.

[17] Ltd. Murata Manufacturing Co., "MBN52832: Bluetooth Low Energy Module," 2017.

[18] ON Semiconductor, “RSL10 SIP: Bluetooth 5 System-in-Package (SiP),” 2018.

[19] Inc. Silicon Laboratories, “BGM220S: BGM220S Wireless Gecko Bluetooth Module,” 2020.

[20] PCBminions, “Typical Specifications,” *https://pcbminions.com/capabilities*. .

[21] Advanced Circuits | 4PCB, “PCB Manufacturing & Assembly Capabilities,” *https://www.4pcb.com/pcb-capabilities.html*. .

[22] San Francisco Circuits, “PCB Production Capabilities,” *https://www.sfcircuits.com/pcb-production-capabilities*. .

[23] Dupont, “Pyralux AC,” *https://www.dupont.com/products/pyralux-ac.html*. .

[24] T. Pattnayak and G. Thanikachalam, “Antenna Design and RF Layout Guidelines,” *Cypress*, no. 001, 2015.

[25] Anil Pandey, “Practical Microstrip and Printed Antenna Design book,” *Artech House USA*, 2019.

[26] S. Drabowitch, A. Papiernik, H. D. Griffiths, J. Encinas, and B. L. Smith, *Modern antennas*. 2005.

[27] T. Taga, K. Tsunekawa, and A. Sasaki, “ANTENNAS FOR DETACHABLE MOBILE RADIO UNITS.,” *Reports of the Electrical Communication Laboratory*, vol. 35, no. 1, 1987.

[28] S. G. Kirtania, A. W. Elger, M. R. Hasan, A. Wisniewska, K. Sekhar, T. Karacolak, and P. K. Sekhar, “Flexible antennas: A review,” *Micromachines*, vol. 11, no. 9. 2020, doi: 10.3390/mi11090847.

[29] J. R. Windmiller and J. Wang, “Wearable Electrochemical Sensors and Biosensors: A Review,” *Electroanalysis*, vol. 25, no. 1. 2013, doi: 10.1002/elan.201200349.

[30] S. Imani, A. J. Bandodkar, A. M. V. Mohan, R. Kumar, S. Yu, J. Wang, and P. P. Mercier, “A wearable chemical-electrophysiological hybrid biosensing system for real-time health and fitness monitoring,” *Nature Communications*, vol. 7, 2016, doi: 10.1038/ncomms11650.

[31] W. Gao, S. Emaminejad, H. Y. Y. Nyein, S. Challa, K. Chen, A. Peck, H. M. Fahad, H. Ota, H. Shiraki, D. Kiriya, D. H. Lien, G. A. Brooks, R. W. Davis, and A. Javey, “Fully integrated wearable sensor arrays for multiplexed in situ perspiration analysis,” *Nature*, vol. 529, no. 7587, 2016, doi: 10.1038/nature16521.

[32] J. Kim, S. Imani, W. R. de Araujo, J. Warchall, G. Valdés-Ramírez, T. R. L. C. Paixão, P. P. Mercier, and J. Wang, “Wearable salivary uric acid mouthguard biosensor with integrated wireless electronics,” *Biosensors and Bioelectronics*, vol. 74, 2015, doi: 10.1016/j.bios.2015.07.039.

[33] D. P. Rose, M. E. Ratterman, D. K. Griffin, L. Hou, N. Kelley-Loughnane, R. R. Naik, J. A. Hagen, I. Papautsky, and J. C. Heikenfeld, “Adhesive RFID sensor patch for monitoring of sweat electrolytes,” *IEEE Transactions on Biomedical Engineering*, vol. 62, no. 6, 2015, doi: 10.1109/TBME.2014.2369991.

[34] A. J. Bandodkar, D. Molinnus, O. Mirza, T. Guinovart, J. R. Windmiller, G. Valdés-Ramírez, F. J. Andrade, M. J. Schöning, and J. Wang, “Epidermal tattoo potentiometric sodium sensors with wireless signal transduction for continuous non-invasive sweat monitoring,” *Biosensors and Bioelectronics*, vol. 54, 2014, doi: 10.1016/j.bios.2013.11.039.

[35] J. Wang, *Analytical Electrochemistry, Third Edition*. 2006.

[36] M. A. Yokus, T. Songkakul, V. A. Pozdin, A. Bozkurt, and M. A. Daniele, “Wearable multiplexed biosensor system toward continuous monitoring of metabolites,” *Biosensors and Bioelectronics*, vol. 153, 2020, doi: 10.1016/j.bios.2020.112038.

[37] M. S. Harrington, L. B. Anderson, J. A. Robbins, and D. H. Karweik, “Multiple electrode potentiostat,” *Review of Scientific Instruments*, vol. 60, no. 10, 1989, doi: 10.1063/1.1140522.

[38] S. S. Ghoreishizadeh, C. Baj-Rossi, A. Cavallini, S. Carrara, and G. de Micheli, "An integrated control and readout circuit for implantable multi-target electrochemical biosensing," *IEEE Transactions on Biomedical Circuits and Systems*, vol. 8, no. 6, 2014, doi: 10.1109/TBCAS.2014.2315157.

[39] A. A. Rowe, A. J. Bonham, R. J. White, M. P. Zimmer, R. J. Yadgar, T. M. Hobza, J. W. Honea, I. Ben-Yaacov, and K. W. Plaxco, "Cheapstat: An open-source, 'do-it-yourself' potentiostat for analytical and educational applications," *PLoS ONE*, vol. 6, no. 9, 2011, doi: 10.1371/journal.pone.0023783.

[40] M. D. M. Dryden and A. R. Wheeler, "DStat: A versatile, open-source potentiostat for electroanalysis and integration," *PLoS ONE*, vol. 10, no. 10, 2015, doi: 10.1371/journal.pone.0140349.

[41] A. Ainla, M. P. S. Mousavi, M. N. Tsaloglou, J. Redston, J. G. Bell, M. T. Fernández-Abedul, and G. M. Whitesides, "Open-Source Potentiostat for Wireless Electrochemical Detection with Smartphones," *Analytical Chemistry*, vol. 90, no. 10, 2018, doi: 10.1021/acs.analchem.8b00850.

[42] S. D. Adams, E. H. Doeven, K. Quayle, and A. Z. Kouzani, "MiniStat: Development and Evaluation of a Mini-Potentiostat for Electrochemical Measurements," *IEEE Access*, vol. 7, 2019, doi: 10.1109/ACCESS.2019.2902575.

[43] O. S. Hoilett, J. F. Walker, B. M. Balash, N. J. Jaras, S. Boppana, and J. C. Linnes, "Kickstat: A coin-sized potentiostat for high-resolution electrochemical analysis," *Sensors (Switzerland)*, vol. 20, no. 8, Apr. 2020, doi: 10.3390/s20082407.

[44] A. Sun, A. G. Venkatesh, and D. A. Hall, "A Multi-Technique Reconfigurable Electrochemical Biosensor: Enabling Personal Health Monitoring in Mobile Devices," *IEEE Transactions on Biomedical Circuits and Systems*, vol. 10, no. 5, 2016, doi: 10.1109/TBCAS.2016.2586504.